Ordered Porphyrin Assemblies

DOI: 10.1002/ange.201409149

Peptide-Induced Hierarchical Long-Range Order and Photocatalytic Activity of Porphyrin Assemblies**

*Kai Liu, Ruirui Xing, Chengjun Chen, Guizhi Shen, Linyin Yan, Qianli Zou, Guanghui Ma, Helmuth Möhwald, and Xuehai Yan**

Abstract: *Long-range structural order and alignment over different scales are of key importance for the regulation of structure and functionality in biology. However, it remains a great challenge to engineer and assemble such complex functional synthetic systems with order over different length scales from simple biologically relevant molecules, such as peptides and porphyrins. Herein we describe the successful introduction of hierarchical long-range order in dipeptide-adjusted porphyrin self-assembly by a thermodynamically driven self-orienting assembly pathway associated with multiple weak interactions. The long-range order and alignment of fiber bundles induced new properties, including anisotropic birefringence, a large Stokes shift, amplified chirality, and excellent photostability as well as sustainable photocatalytic activity. We also demonstrate that the aligned fiber bundles are able to induce the epitaxially oriented growth of Pt nanowires in a photocatalytic reaction.*

Self-assembly is ubiquitous at various length scales throughout biology and is a key process of life. Structural complexity in biological systems stems from the hierarchically ordered organization of molecular elements (such as amino acids, peptides, proteins, lipids, and nucleic acids) on the basis of intermolecular noncovalent interactions, including electrostatic, hydrogen-bonding, π–π, van der Waals, and hydrophobic interactions.[1,2] Inspired largely by biological systems, bottom-up self-assembly has been developed as an elegant strategy for the synthesis of a rich variety of functional high-order structures and materials. Over the past decade, significant progress has been made, and a number of fascinating nanostructures, such as nanotubes, vesicles, micelles, nanofibers, and nanorods, have been synthesized by the self-assembly of molecular building blocks, including peptides and proteins.[3] These well-defined nanostructures could be considered as an assembly of molecules into supramolecular systems at the nanoscale.

However, a great challenge remains to design and create complex functional systems analogous to biological systems, with long-range alignment of molecules over different scales in a hierarchically organized manner in aqueous media. The bundling and orientation of nanoscale substructures preformed from molecular building blocks (such as actin filaments and microtubules, which are ubiquitous in living cells) regulate cellular events, including mitosis, substance transport, and signal transduction.[4] That is, long-range structural order beyond the nanoscale is essential in biological systems for regulating structure and enabling functionality. Therefore, processes for the creation of hierarchical long-range structural order of biologically relevant molecules (such as peptides and porphyrins) by self-assembly and insight into the organization mechanisms are of crucial importance for directing the construction of complex synthetic systems with multiple functional properties. We report herein the discovery of a self-orienting assembly pathway in the solution phase that leads porphyrin J-aggregates to form fiber bundles that are highly aligned over long distances owing to the peptide-mediated adjustment of intermolecular synergistic interactions in association with electrostatic, π–π, hydrogen-bonding and van der Waals forces.

One of the key types of naturally occurring biomolecules are porphyrins, a main component of light-harvesting systems in both photosynthetic bacteria and green plants.[5] In a biological setting, porphyrin molecules function as a result of their organization by means of peptides or proteins and other molecules, but not individually.[6] In this study, the highly ordered organization and concomitant long-range alignment of the negatively charged porphyrin molecule (tetrakis(4-sulfonatophenyl)porphine (H_2TPPS; see Figure S1 in the Supporting Information)[7] was induced by a simple positively charged dipeptide (L-Lys-L-Lys, KK; see Figure S1) through tuned self-assembly in solution. We demonstrate that nanorod-shaped J-aggregates, formed preferentially by strong π–π interactions of H_2TPPS molecules, spontaneously group into aligned fiber bundles, presumably as a result of the compromise between long-range electrostatic repulsion and short-range van der Waals attraction. The bundled fibers are anisotropically aligned and show amplified

[*] Dr. K. Liu, R. Xing, Dr. C. Chen, Dr. G. Shen, Dr. L. Yan, Dr. Q. Zou, Prof. Dr. G. H. Ma, Prof. Dr. X. Yan
National Key Laboratory of Biochemical Engineering
Institute of Process Engineering, Chinese Academy of Sciences
100190 Beijing (China)
E-mail: yanxh@ipe.ac.cn
Homepage: http://www.yan-assembly.org/
Dr. K. Liu
University of Chinese Academy of Sciences
Beijing 100049 (China)
Dr. G. Shen, Prof. Dr. H. Möhwald
Max Planck Institute of Colloids and Interfaces
Am Mühlenberg 1, 14476 Potsdam/Golm (Germany)

[**] We acknowledge financial support from the National Nature Science Foundation of China (Project Nos. 21473208, 81402871, and 51403214), the Talent Fund of the Recruitment Program of Global Youth Experts, the Chinese Academy of Sciences (CAS), and CAS visiting professorships for senior international scientists (Project No. 2013T2G0037) as well as the German Max Planck Society. The first two authors contributed equally to this work.

Supporting information for this article is available on the WWW under http://dx.doi.org/10.1002/anie.201409149.

chirality, a large Stokes shift, and excellent photostability. Significantly, the bundling and long-range alignment of nanoscale J-aggregates support sustainable photocatalytic reactions and remain stable against photodegradation, in contrast to individual H_2TPPS J-aggregates. This finding will enable the self-assembly of sophisticated functional systems with hierarchically organized structures over different scales in the solution phase through the tuning of intermolecular synergistic interactions and could potentially extend the range of robust structures and functional properties known for these materials.

We observed the immediate appearance of visible green aggregates as negatively charged H_2TPPS was mixed with positively charged KK at a final pH value smaller than 2 in an aqueous solution. Scanning electron microscopy (SEM) and transmission electron microscopy (TEM) showed that the aggregates were long fiber bundles consisting of orientationally aligned nanorod and/or nanofiber substructures (Figure 1 a,b; see also Figure S2). The fiber bundles had widths of several micrometers and lengths of tens of micrometers (up to

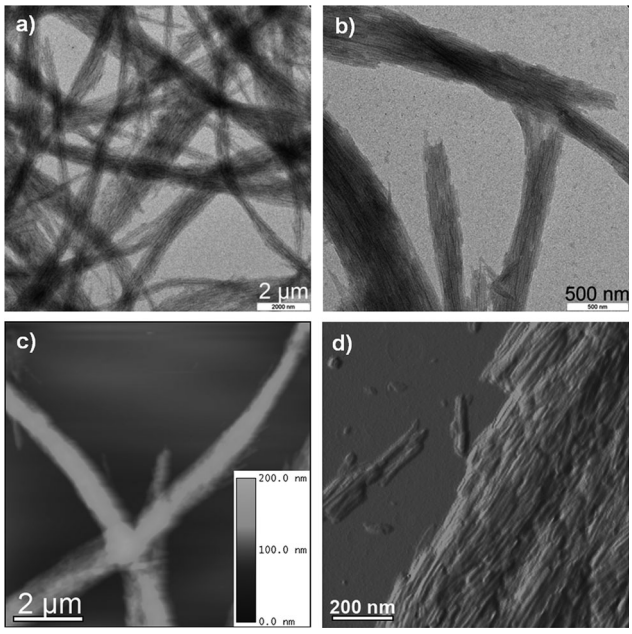

Figure 1. a) TEM image of bundled fibers. b) Magnified TEM image of the fibers, showing aligned substructures at long range. c) AFM contact-mode height image of bundled fibers (the top value on the scale is 200 nm; the bottom value is 0 nm). d) Magnified AFM amplitude image of a single fiber showing the long-range order of aligned nanorods or nanofibers along the longitudinal axis.

hundreds of micrometers). This observed structure is rather different from the organized structure of H_2TPPS J-aggregates, which are well known to form nanorods and nanoribbons with a typical width and length of 20–30 nm and several micrometers,[8] respectively, as also confirmed by SEM (see Figure S2 b). Atomic force microscopy (AFM) of the surface of single fiber bundles confirmed the presence of aligned nanorods and nanofibers of tens of nanometers in diameter along the long axis of the fiber bundles (Figure 1 c,d), in agreement with the SEM and TEM observation. These hierarchically organized structures of photosynthetic molecules are reminiscent of complex functional systems in biology, such as the natural light-harvesting antennae (chlorosomes) of green sulfur bacteria, which are a typical class of photosynthetic bacteria living in deep oceans.[9] The chlorosomes are an ensemble of light-harvesting pigments with hierarchically organized structures featuring long-range alignment. These structures enable efficient light harvesting and offer protection from photodegradation. Higher-level order of photosynthetic porphyrin assemblies possibly leads to the amplification of characteristic spectroscopic signatures and improvement of the corresponding photocatalytic activity.

J-Aggregates of H_2TPPS molecules have a UV/Vis absorption spectrum with a strongly red shifted Soret band at 490 nm (J-band) as compared to that of H_2TPPS monomers, and a second band at 705 nm (Q-band; Figure 2 a). H_2TPPS monomers have corresponding absorptions at 434 and 645 nm (see Figure S3).[10] The fiber bundles showed a spectroscopic signature similar to that of J-aggregates alone, but with apparent broadening of both the Soret band and the Q-band. This result indicates interactions between KK dipeptides and H_2TPPS. The spectral broadening is probably caused by the change in polarity around the assembled porphyrins in the presence of positively charged dipeptides.[11] The Fourier transform infrared (FTIR) spectrum of the H_2TPPS J-aggregates showed strong bands at 1226 and 1192 cm^{-1}, which are attributed to the vibrations of SO_3^- groups. These bands shifted to 1221 and 1181 cm^{-1}, respectively, in the case of the fiber bundles (see Figure S4). This shift indicates strong interactions between KK dipeptides and H_2TPPS, presumably as a result of hydrogen bonding and electrostatic interactions. Circular dichroism (CD) spectroscopic analysis showed that the fiber bundles had a strongly split Cotton effect with positive and negative signals at 486 and 493 nm, respectively, and the signal intensity was 10 times that observed for individual J-aggregates (Figure 2 b).[7] This result indicates that the chiral signature of organized porphyrins is dramatically amplified as a result of peptide-induced hierarchical long-range alignment. Time-dependent CD spectra gave in-depth insight into structure formation and evolution (see Figure S5). It was found that the CD peaks in the first 5 min after H_2TPPS was mixed with KK were ill-defined, after 15 min they became normal, and the intensity of the chiral signal increased markedly over time. This observation suggests a dipeptide-induced growth of J-aggregates associated with the charge screening of H_2TPPS, which in turn promotes helical packing in the peptide–porphyrin nanorods/nanofibers. The ill-defined chiral signature implies initially incomplete formation of J-aggregates, presumably owing to the strong interactions between KK and H_2TPPS monomers or oligomers, thus influencing the ordered stacking of H_2TPPS units in the helices. Nevertheless, assembly into a helical-packing arrangement predominates over time, and J-aggregate nanorods ultimately form through dynamic regulation by balancing electrostatic, hydrogen-bonding, and π–π interactions. The nanoscale substructures further self-assemble to form fiber bundles with long-range order, as evidenced by signal amplification in the CD spectrum and microscopic observations.

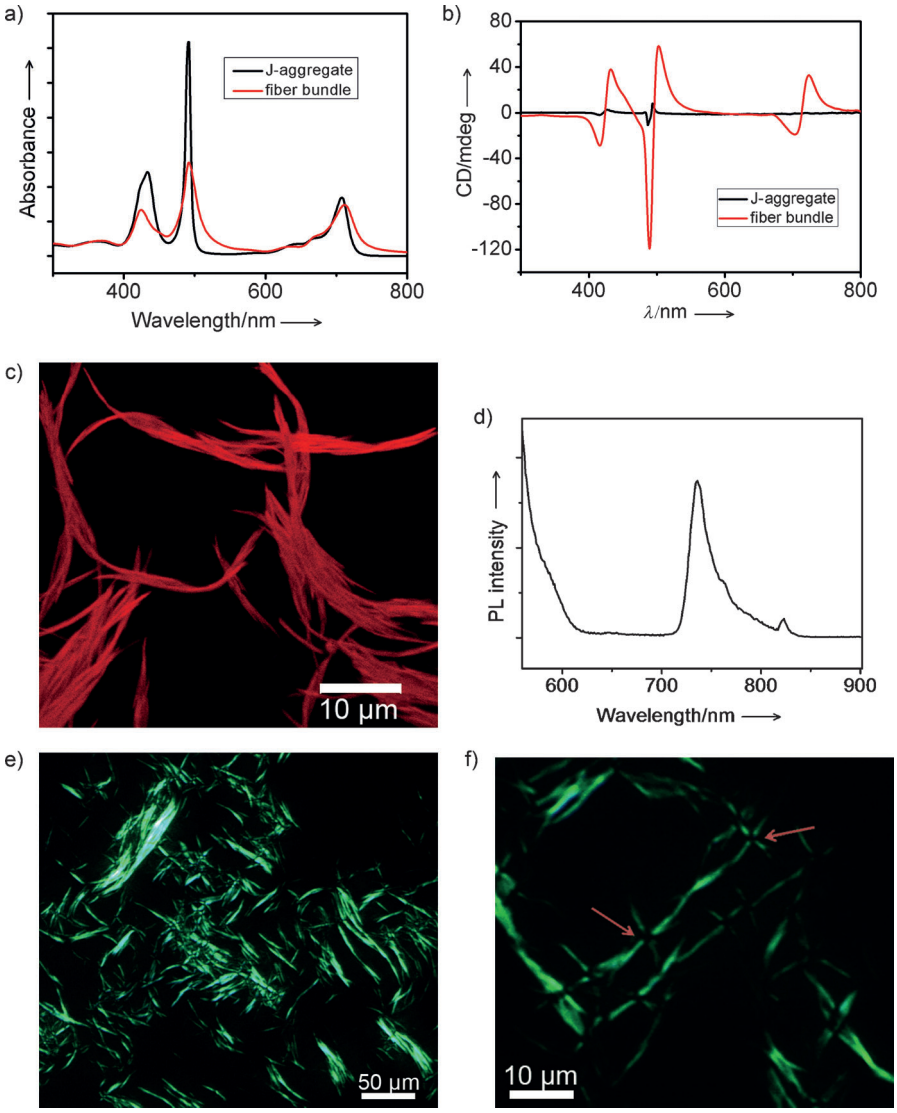

Figure 2. a) UV/Vis absorption spectra of J-aggregates (stacked H_2TPPS) formed at pH 1.9 and fiber bundles self-assembled through the electrostatic coupling of cationic KK and anionic H_2TPPS. b) CD spectra of H_2TPPS J-aggregates and fiber bundles showing a strongly split Cotton effect and a 10-fold higher signal intensity of the fiber bundles relative to that of the J-aggregates. c) Confocal image of fiber bundles showing red photoluminescence. The fiber sample was excited at 488 nm and the emitted fluorescence collected from 680 to 760 nm. d) Fluorescence spectrum of peptide–porphyrin fiber bundles showing an emission maximum at 720 nm. The sample was excited at 488 nm. e) Birefringence of fiber bundles between crossed polarizers. This effect suggests an ordered alignment along the longitudinal axis. f) Extinction of anisotropic photoluminescence (as denoted by arrows) at the cross-points of orthogonal fiber bundles under crossed polarizers. This effect indicates a uniform distribution of aligned substructures in each fiber.

Confocal fluorescence microscopy images showed red fluorescence of fiber bundles upon excitation at 488 nm that is attributable to the presence of porphyrins within the fiber bundles (Figure 2c). The fluorescence spectrum of the fiber bundles showed an emission maximum at 720 nm (excitation at 488 nm; Figure 2d). This result is consistent with the observation of red fluorescence by confocal fluorescence microscopy. Apparently, the bundling leads to a large Stokes shift of more than 200 nm. This Stokes shift may enhance photostability. Strong birefringence was observed throughout the fiber bundles when they were located between crossed polarizers (Figure 2e,f). This result indicates that the order extends from the molecular level to the nanoscale and even to the microscale within the hierarchically organized fiber bundles. Birefringence extinction at the cross-point of two orthogonal fiber bundles observed by polarized microscopy indicates the uniform distribution of aligned nanorods/nanofibers in each.

On the basis of these results, we are able to suggest a mechanism for the formation of fiber bundles (Figure 3). Nanorods consisting of J-aggregates are initially formed as a consequence of dipeptide-mediated charge screening of porphyrin J-aggregates in combination with hydrogen-bonding and π-stacking interactions. The induction of J-aggregate formation by cationic KK was further confirmed by the following control experiments. It is well-known that H_2TPPS can generally form J-aggregates at pH < 2.[12] In the present case, the fiber bundles were exclusively observed at a pH values higher than 3.9 (see Figure S6), thus indicating the dominant role of cationic KK in triggering the onset of J-aggregate formation and facilitating the subsequent assembly of fiber bundles. By contrast, shorter fibers similar to H_2TPPS J-aggregates were formed when the hydrophobic naphthalene-modified dilysine H-Lys-Lys-βNA (KK-βNA; see Figure S1) was used instead of KK for coassembly (see Figure S7), because the hydrophobic group naphthalene to some extent engages in π-stacking with porphyrin molecules, thus influencing the long-range order based on π–π stacking and hydrogen bonding. The formed nanorods spontaneously align at long range, presumably by a self-orienting assembly process due to the competition of rotational and translational entropy in terms of Onsager theory.[13] The rapid growth and formation of nanorods leads to a high local concentration of nanorods, thus promoting orientation and alignment at long range. In the absence of dipeptides, the concentration of J-aggregate nanorods is relatively low, and the nanorods can move freely in the diluted suspension without restriction by neighboring nanorods, thus enabling the random orientation of nanorods and maximizing the rotational and translational entropy. In the case of the

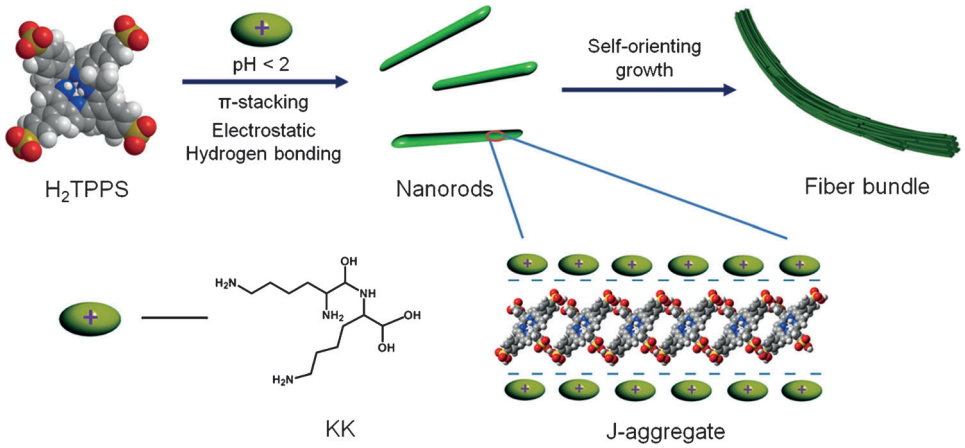

Figure 3. Proposed mechanism for the formation of fiber bundles at long range: Nanorods consisting of J-aggregates are initially formed as a consequence of the dipeptide-mediated charge screening of porphyrin J-aggregates in combination with hydrogen-bonding and π-stacking interactions. The formed nanorods spontaneously align at long range, presumably by a self-orienting assembly process due to competition between long-range electrostatic repulsion and short-range van der Waals attraction.

dipeptide-induced formation of fiber bundles, the nanorods grow rapidly and are confined in a limited space; their translational freedom is limited. The total entropy is maximized through the alignment of the nanorods: The translational entropy is increased by sacrificing the orientational entropy.

The ordered alignment of nanorods into higher-level superstructures (bundles) is astonishing and of key importance for improving the functional properties of such materials, such as photocatalytic activity and photostability. For the first proof-of-concept study, we compared the light-induced oxidation of iodide to triiodide in the presence of fiber bundles and individual J-aggregates. The bands at $\lambda = 353$ and 287 nm in the UV/Vis absorption spectra correspond to the characteristic absorption of triiodide,[6b,14] the time-dependent production of which can be used to monitor the reaction rate related to photocatalytic activity (Figure 4a). The photocatalytic oxidation reaction was supported in the presence of the fiber bundles, as confirmed by the increase in the peak intensities at $\lambda = 353$ nm and 287 nm. The absorption intensity at $\lambda = 353$ nm was plotted as a function of time to study the kinetic evolution of triiodide (Figure 4b). In comparison to the use of individual J-aggregates, the reaction rate with the fiber bundles is rather low at the beginning of the reaction, but increases more rapidly after 2 h and retains the rising tendency with time. The lower reaction rate at the beginning may be attributed to the higher-level assembly of dipeptide-mediated porphyrin J-aggregates.

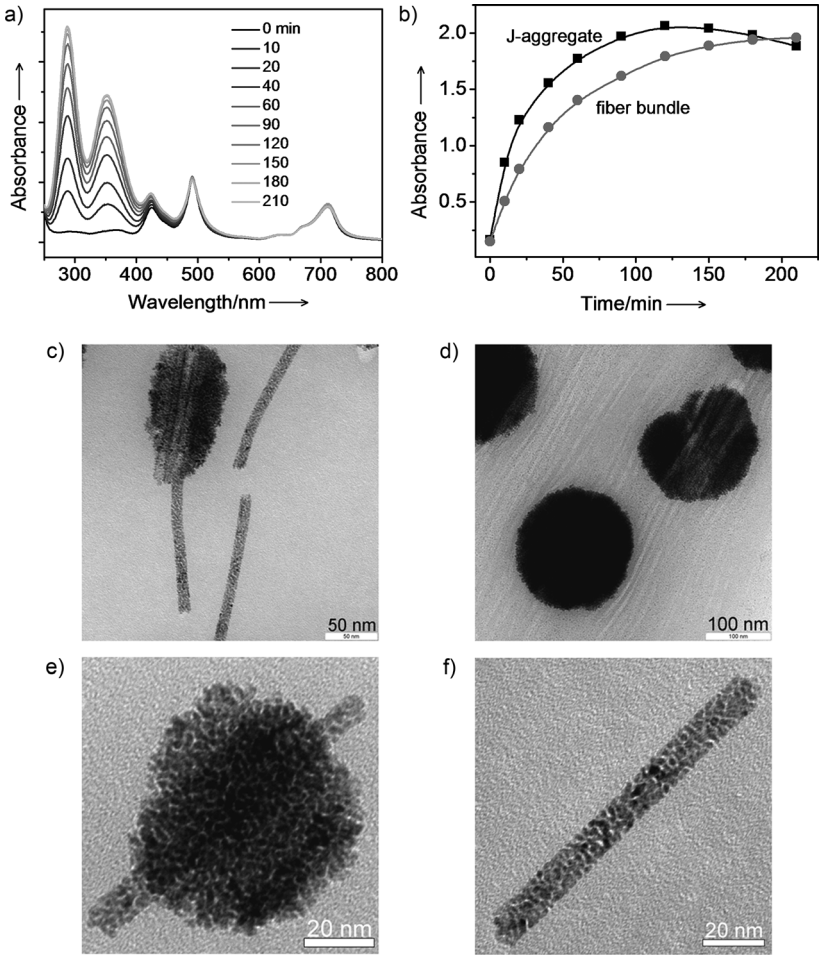

Figure 4. a) UV/Vis absorption spectra quantifying the photocatalytic synthesis of triiodide by fiber bundles and showing time-dependent changes in the peak intensities at $\lambda = 353$ nm and 287 nm (initial iodide concentration is 5 mM). b) Plots of absorption intensity ($\lambda = 353$ nm) versus irradiation time for triiodide production in the presence of fiber bundles or H_2TPPS J-aggregates. c,d) TEM images of Pt nanowires and nanospheres synthesized in situ in the presence of fiber bundles by a photocatalytic pathway. e,f) Magnified TEM images of a Pt nanowire and nanosphere surrounding the nanowire.

It is self-evident that the catalytic accessible surface of the fiber bundles is smaller than that of J-aggregate nanorods (AFM images) for the same porphyrin concentration, thus explaining why the reaction rate with fiber bundles is lower in the initial stage of the reaction. However, pure J-aggregates are not stable enough against photodegradation, thus leading to a decay in photocatalytic activity with time. In contrast, the higher-level organization of fiber bundles enables more efficient resistance against light damage, as evidenced by the

negligible change in peak intensity of both the Soret band and the Q-band. Hence, the higher-order organization of dipeptide-induced porphyrin supramolecular stacking is probably responsible for the enhanced photocatalytic performance.

Their photocatalytic properties make the hierarchically organized fiber bundles a most suitable photocatalytic template for the in situ synthesis of functional metal nanoparticles with high potential for a broad range of applications. Therefore, we investigated the feasibility of the use of peptide–porphyrin fiber bundles to capture visible light for the photocatalytic synthesis of PtNPs in the presence of ascorbic acid as an electron donor (Figure 4c–f; see also Figure S8). It was evident that Pt nanospheres with a diameter of 100–200 nm or nanowires of around 200 nm in length and 10 nm in width were formed locally on the fiber bundles. Magnified TEM images indicated that both nanospheres and nanowires comprised individual nanoparticles of approximately 2 nm in size (Figure 4c,d). Control experiments without light irradiation or in the absence of the fiber bundles showed no production of such Pt nanostructures, thus indicating that the photocatalytic process takes place in the presence of the fiber bundles. These results suggest that porphyrins within the fiber bundles efficiently capture light to yield photoexcited states that are rapidly reduced by ascorbic acid (electron donor). The resulting porphyrin radical anion has rather strong reduction capability. Thus, metal salts are catalytically reduced to the metallic state through a succession of light-harvesting and photochemical cycles.[15] The growth of Pt nanospheres appears to be directly related to the nanowires that were commonly observed if the concentration of Pt salts or the aging time was reduced (see Figure S9). Apparently, the nanospheres prefer to grow around the nanowires (Figure 4e), presumably as a result of further growth through an autocatalytic reduction process.[15b] Surprisingly, the Pt nanowires were exclusively oriented along the longitudinal axis of the fiber bundles and had a uniform diameter, thus suggesting an epitaxial growth mechanism along the texture of the aligned fibers. The formation of nanowires most likely follows a photocatalytic reduction mechanism, as the nanowires consist of relatively discrete PtNPs with size of about 2 nm (Figure 4f). Overall, photosynthetic fiber bundles can serve as biotemplates for directing the synthesis of functional metal nanostructures through a predominantly photocatalytic reduction mechanism. In particular, the hierarchical long-range alignment within the fiber bundles induces the epitaxial growth and orientation of Pt nanowires.

In conclusion, we have demonstrated that the dipeptide-adjusted self-assembly of porphyrin molecules can lead to the highly ordered organization and long-range alignment of nanorod-shaped porphyrin J-aggregates. Competitive multiple weak interactions, such as electrostatic, π–π, hydrogen-bonding, and van der Waals interactions, are responsible for the hierarchical organization and order at different length scales. We propose a self-orienting assembly pathway as described by Onsager theory for the formation of the fiber bundles. The hierarchical long-range alignment into fiber bundles introduces the new properties of anisotropic birefringence, a large Stokes shift, amplified helicity, and excellent photostability. We have also demonstrated that the fiber bundles support sustainable photocatalytic reactions and perform better than isolated porphyrin J-aggregates. The long-range alignment induces the unique epitaxially oriented growth of Pt nanowires (ultimately into Pt nanospheres) consisting of discrete Pt nanoparticles of 2 nm in size in a photocatalytic process. The coassembly of biologically relevant small molecules, such as dipeptides and photosensitized dyes, into superstructures with long-range order and insight into their organization mechanism will offer a reference for the design and engineering of biomimetic multifunctional complex systems from simple molecular building blocks. Furthermore, our findings unravel the potential of the long-range alignment of fibers into bundles for the design of molecular materials and devices with new functions and properties.

Received: September 16, 2014
Revised: October 7, 2014
Published online: November 5, 2014

Keywords: fiber bundles · hierarchical long-range order · peptides · porphyrinoids · self-assembly

[1] a) J.-M. Lehn, *Proc. Natl. Acad. Sci. USA* **2002**, *99*, 4763–4768; b) G. M. Whitesides, B. Grzybowski, *Science* **2002**, *295*, 2418–2421; c) T. Aida, E. W. Meijer, S. I. Stupp, *Science* **2012**, *335*, 813–817; d) P. A. Korevaar, S. J. George, A. J. Markvoort, M. M. J. Smulders, P. A. J. Hilbers, A. P. H. J. Schenning, T. F. A. De Greef, E. W. Meijer, *Nature* **2012**, *481*, 492–496; e) S. F. M. van Dongen, S. Cantekin, J. A. A. W. Elemans, A. E. Rowan, R. J. M. Nolte, *Chem. Soc. Rev.* **2014**, *43*, 99–122; f) Y. S. Xie, M. Akada, J. P. Hill, Q. M. Ji, R. Charveta, K. Ariga, *Chem. Commun.* **2011**, *47*, 2285–2287; g) M. Li, S. Ishihara, Q. Ji, M. Akada, J. P. Hill, K. Ariga, *Sci. Technol. Adv. Mater.* **2012**, *13*, 053001.

[2] a) J. B. Li, Q. He, X. H. Yan, *Molecular Assembly of Biomimetic Systems*, Wiley, Hoboken, **2011**; b) S. Mann, *Acc. Chem. Res.* **2012**, *45*, 2131–2141; c) Q. L. Zou, L. Zhang, X. H. Yan, A. H. Wang, G. H. Ma, J. L. Li, H. Möhwald, S. Mann, *Angew. Chem. Int. Ed.* **2014**, *53*, 2366–2370; *Angew. Chem.* **2014**, *126*, 2398–2402; d) F. F. Zhao, G. Z. Shen, C. J. Chen, R. R. Xing, Q. L. Zou, G. H. Ma, X. H. Yan, *Chem. Eur. J.* **2014**, *20*, 6880–6887.

[3] a) K. Ariga, Q. M. Ji, T. Mori, M. Naito, Y. Yamauchi, H. Abe, J. P. Hill, *Chem. Soc. Rev.* **2013**, *42*, 6322–6345; b) M. A. Kostiainen, O. Kasyutich, J. J. L. M. Cornelissen, R. J. M. Nolte, *Nat. Chem.* **2010**, *2*, 394–399; c) R. V. Ulijn, D. N. Woolfson, *Chem. Soc. Rev.* **2010**, *39*, 3349–3350, and references therein; d) X. H. Yan, P. L. Zhu, J. B. Li, *Chem. Soc. Rev.* **2010**, *39*, 1877–1890; e) X. H. Yan, J. B. Li, H. Möhwald, *Adv. Mater.* **2011**, *23*, 2796–2801; f) X. H. Yan, Y. Su, J. B. Li, J. Früh, H. Möhwald, *Angew. Chem. Int. Ed.* **2011**, *50*, 11186–11191; *Angew. Chem.* **2011**, *123*, 11382–11387; g) L. Adler-Abramovicha, E. Gazit, *Chem. Soc. Rev.* **2014**, DOI: 10.1039/c4s00164h; h) S. G. Zhang, *Nat. Biotechnol.* **2003**, *21*, 1171–1178.

[4] a) D. J. Needleman, M. A. Ojeda-Lopez, U. Raviv, H. P. Miller, L. Wilson, C. R. Safinya, *Proc. Natl. Acad. Sci. USA* **2004**, *101*, 16099–16103; b) H. G. Cui, E. T. Pashuck, Y. S. Velichko, S. J. Weigand, A. G. Cheetham, C. J. Newcomb, S. I. Stupp, *Science* **2010**, *327*, 555–559; c) S. Zhang, M. A. Greenfield, A. Mata, L. C. Palmer, R. Bitton, J. R. Mantei, C. Aparicio, M. O. de La Cruz, S. I. Stupp, *Nat. Mater.* **2010**, *9*, 594–601.

[5] a) C. M. Drain, A. Varotto, I. Radivojevic, *Chem. Rev.* **2009**, *109*, 1630–1658; b) F. Würthner, T. E. Kaiser, C. R. Saha-Möller,

Angew. Chem. Int. Ed. **2011**, *50*, 3376 – 3410; *Angew. Chem.* **2011**, *123*, 3436 – 3473; c) T. Silviu Balaban, *Acc. Chem. Res.* **2005**, *38*, 612 – 623.

[6] a) D. E. Wagner, C. L. Phillips, W. M. Ali, G. E. Nybakken, E. D. Crawford, A. D. Schwab, W. F. Smith, R. Fairman, *Proc. Natl. Acad. Sci. USA* **2005**, *102*, 12656 – 12661; b) S. Frühbeißer, F. Gröhn, *J. Am. Chem. Soc.* **2012**, *134*, 14267 – 14270; c) B. C. Kovaric, B. Kokona, A. D. Schwab, M. A. Twomey, J. C. de Paula, R. Fairman, *J. Am. Chem. Soc.* **2006**, *128*, 4166 – 4167.

[7] J. M. Ribó, J. Crusats, F. Sagués, J. Claret, R. Rubires, *Science* **2001**, *292*, 2063 – 2066.

[8] a) O. Ohno, Y. Kaizu, H. Kobayashi, *J. Chem. Phys.* **1993**, *99*, 4128 – 4139; b) L. Zhang, M. H. Liu, *J. Phys. Chem. B* **2009**, *113*, 14015 – 14020; c) A. D. Schwab, D. E. Smith, C. S. Rich, E. R. Young, W. F. Smith, J. C. de Paula, *J. Phys. Chem. B* **2003**, *107*, 11339 – 11345.

[9] a) S. Ganapathy, G. T. Oostergetel, P. K. Wawrzyniak, M. Reus, A. Gomez Maqueo Chew, F. Buda, E. J. Boekema, D. A. Bryant, A. R. Holzwarth, H. J. M. de Groot, *Proc. Natl. Acad. Sci. USA* **2009**, *106*, 8525 – 8530; b) J. W. Schopf, A. B. Kudryavtsev, A. D. Czaja, A. B. Tripathi, *Precambrian Res.* **2007**, *158*, 141 – 155; c) S. Mann, *Angew. Chem. Int. Ed.* **2013**, *52*, 155 – 162; *Angew. Chem.* **2013**, *125*, 166 – 173.

[10] a) E. B. Fleischer, J. M. Palmer, T. Srivastava, A. Chatterjee, *J. Am. Chem. Soc.* **1971**, *93*, 3162 – 3167; b) R. F. Pasternack, P. R. Huber, P. Boyd, G. Engasser, L. Francesconi, E. Gibbs, P. Fasella, G. Cerio Venturo, L. d. Hinds, *J. Am. Chem. Soc.* **1972**, *94*, 4511 – 4517; c) B. J. Pepe-Mooney, B. Kokona, R. Fairman, *Biomacromolecules* **2011**, *12*, 4196 – 4203.

[11] D. Mauzerall, *Biochemistry* **1965**, *4*, 1801 – 1810.

[12] B. Kokona, A. M. Kim, R. C. Roden, J. P. Daniels, B. J. Pepe-Mooney, B. C. Kovaric, J. C. de Paula, K. A. Johnson, R. Fairman, *Biomacromolecules* **2009**, *10*, 1454 – 1459.

[13] L. Onsager, *Ann. N. Y. Acad. Sci.* **1949**, *51*, 627 – 659.

[14] L. Slavětínská, J. Mosinger, P. Kubát, *J. Photochem. Photobiol. A* **2008**, *195*, 1 – 9.

[15] a) J. Song, Y. Yang, C. J. Medforth, E. Pereira, A. K. Singh, H. F. Xu, Y. B. Jiang, C. J. Brinker, F. van Swol, J. A. Shelnutt, *J. Am. Chem. Soc.* **2004**, *126*, 635 – 645; b) Z. C. Wang, C. J. Medforth, J. A. Shelnutt, *J. Am. Chem. Soc.* **2004**, *126*, 16720 – 16721.

